



1 **Contrasting responses of phytoplankton productivity between coastal and offshore**
2 **surface waters in the Taiwan Strait and the South China Sea to future CO₂-induced**
3 **acidification**

4

5 Guang Gao¹, Tifeng Wang¹, Jiazhen Sun¹, Xin Zhao¹, Lifang Wang¹, Xianghui Guo¹,
6 Kunshan Gao^{1,2*}

7 ¹State Key Laboratory of Marine Environmental Science & College of Ocean and Earth
8 Sciences, Xiamen University, Xiamen 361005, China

9 ²Co-Innovation Center of Jiangsu Marine Bio-industry Technology, Jiangsu Ocean
10 University, Lianyungang 222005, China

11

12 *Corresponding author: ksgao@xmu.edu.cn

13



14 **Abstract**

15 Future CO₂-induced ocean acidification (OA) has been documented to either inhibit or
16 enhance or result in no effect on marine primary productivity (PP). In order to examine
17 effects of OA under multiple drivers, we investigated the influences of OA (a decrease of
18 0.4 pH_{total} units with corresponding CO₂ concentrations ranged 22.0-39.7 μM) on PP
19 through deck-incubation experiments at 101 stations in the Taiwan Strait and the South
20 China Sea (SCS), including the coastal zone, the continental shelf and slope, as well as
21 deep-water basin. The daily net primary productivities in surface seawater under incident
22 solar radiation ranged from 17-306 μg C (μg Chl *a*)⁻¹ d⁻¹, with the responses of PP to OA
23 being region-dependent and the OA-induced changes varying from -88.03% (inhibition)
24 to 56.87% (enhancement). The OA-treatment stimulated PP in surface waters of coastal,
25 estuarine and shelf waters, but suppressed it in the South China Sea basin. Such
26 OA-induced changes in PP were significantly related to NO_x (the sum of NO₃⁻ and NO₂⁻)
27 availability, in situ pH and solar radiation in surface seawater, but negatively related to
28 salinity changes. Our results indicate that phytoplankton cells are more vulnerable to pH
29 drop in oligotrophic waters. Considering high nutrient and low salinity in coastal waters
30 and reduced nutrient availability in pelagic zones with the progressive stratification
31 associated with ocean warming, our results imply that future OA will enhance PP in
32 coastal waters but decrease it in pelagic oligotrophic zones.

33 **Keywords:** CO₂; Taiwan Strait; ocean acidification; photosynthesis; primary productivity;



34 South China Sea

35 **1 Introduction**

36 The oceans have absorbed about one-third of anthropogenically released CO₂, which
37 increased dissolved CO₂ and decreased pH of seawater (Gattuso et al., 2015), leading to
38 ocean acidification (OA). OA has been shown to result in profound influences on marine
39 ecosystems (see the reviews and literature therein, Mostofa et al., 2016; Doney et al.,
40 2020). Marine photosynthetic organisms, which contribute about half of the global
41 primary production, are also being affected by OA (see the reviews and literatures therein,
42 Riebesell et al., 2018; Gao et al., 2019a). It is of general concern that the oceans are going
43 to take more or less CO₂ with progressive OA, since the amount of CO₂ uptake by the
44 oceans is essential to predict global and ocean warming trends. Therefore, it is important
45 to understand the responses of the key players of marine biological CO₂ pump, the
46 phytoplankton, to OA and other climate change drivers.

47 Elevated CO₂ is well recognized to lessen the dependence of algae and
48 cyanobacteria on energy-consuming CO₂ concentrating mechanisms (CCMs) which
49 concentrate CO₂ around Rubisco, the key site for photosynthetic carbon fixation (Raven
50 & Beardall, 2014 and references therein; Hennon et al., 2015). The energy freed up from
51 the down-regulated CCMs under increased CO₂ concentrations can be applied to other
52 metabolic processes, resulting in a modest increase in algal growth (Wu et al., 2010;
53 Hopkinson et al., 2011; Xu et al., 2017). Accordingly, elevated CO₂ availability could



54 potentially enhance marine primary productivity (Schippers et al., 2004). For instance,
55 across 18 stations in the central Atlantic Ocean primary productivity was stimulated by
56 15-19% under elevated dissolved CO₂ concentrations up to 36 μM (Hein and
57 Sand-Jensen 1997). On the other hand, neutral effects of OA on growth rates of
58 phytoplankton communities were reported in five of six CO₂ manipulation experiments in
59 the coastal Pacific (Tortell et al., 2000). Furthermore, simulated future OA reduced
60 surface PP in pelagic surface waters of Northern SCS and East China Sea (Gao et al.,
61 2012). It seems that the impacts of OA on PP could be region-dependent. The varying
62 effects of OA may be related to the regulation of other factors such as light intensity (Gao
63 et al., 2012), temperature (Holding et al., 2015), nutrients (Tremblay et al., 2006) and
64 community structure (Dutkiewicz et al., 2015).

65 Taiwan Strait of the East China Sea, located between southeast Mainland China and
66 the Taiwan Island, is an important channel in transporting water and biogenic elements
67 between the East China Sea (ECS) and the South China Sea (SCS). Among the Chinese
68 coastal areas, the Taiwan Strait is distinguished by its unique location. In addition to
69 riverine inputs, it also receives nutrients from upwelling (Hong et al., 2011). Primary
70 productivity is much higher in coastal waters than that in pelagic zones due to increased
71 supply of nutrients through river runoff and upwelling (Chen, 2003; Cloern et al., 2014).
72 The South China Sea (SCS), located from the equator to 23.8° N, from 99.1 to 121.1° E
73 and encompassing an area of about 3.5×10^6 km², is one of the largest marginal seas in



74 the world. As a marginal sea of the Western Pacific Ocean, it has a deep semi-closed
75 basin (with depths > 5000 m) and wide continental shelves, characterized by a tropical
76 and subtropical climate (Jin et al., 2016). Approximately 80% of ocean organic carbon is
77 buried in the Earth's continental shelves and therefore continental margins play an
78 essential role in the ocean carbon cycle (Hedges & Keil, 1995). Investigating how ocean
79 acidification affects primary productivity in the Taiwan Strait and the SCS could help us
80 to understand the contribution of marginal seas to carbon sink under the future
81 CO₂-increased scenarios. Although small-scale studies on OA impacts have been
82 conducted in the ESC and the SCS (Gao et al., 2012, 2017), our understanding of how
83 OA affects PP in marginal seas is still fragmentary and superficial. In this study, we
84 conducted three cruises in the Taiwan Strait and the SCS, covering an area of 8.3×10^5
85 km², and aimed to provide in-depth insight into how OA and/or episodic pCO₂ rise
86 affects PP in marginal seas with comparisons to other types of waters.

87 **2 Materials and Methods**

88 **2.1 Investigation areas**

89 To study the impacts of projected OA (dropping by ~0.4 pH) on marine primary
90 productivity in different areas, we carried out deck-based experiments during the 3
91 cruises supported by National Natural Science Foundation of China (NSFC), which took
92 place in the Taiwan Strait (Jul 14th-25th, 2016), the South China Sea basin (Sep 6-24th,
93 2016), and the West South China Sea (Sep 14th to Oct 24th, 2017), respectively. The



94 experiments were conducted at 101 stations with coverage of 12 °N-26 °N and 110
95 °E-120 °E (Fig. 1). Investigation areas include the coastal zone (< 50 m), the continental
96 shelf (50-200 m) and the slope (200-1000 m), and the vast deep-water basin (> 1000 m).

97 **2.2 Measurements of temperature and carbonate chemistry parameters**

98 The temperature and salinity of surface seawater at each station were monitored with
99 an onboard CTD (Seabird, USA). pH_{NBS} was measured with an Orion 2-Star pH meter
100 (Thermo scientific, USA) that was calibrated with standard National Bureau of Standards
101 (NBS) buffers ($\text{pH}=4.01, 7.00, \text{ and } 10.01$ at $25.0\text{ }^{\circ}\text{C}$; Thermo Fisher Scientific Inc., USA).
102 The analytical precision was ± 0.001 . Total alkalinity (TALK) was determined using Gran
103 titration on a 25-mL sample with a TA analyzer (AS-ALK1, Apollo SciTech, USA) that
104 was regularly calibrated with certified reference materials supplied by A. G. Dickson at
105 the Scripps Institution of Oceanography (Gao et al., 2018a). The analytical precision was
106 $\pm 2\text{ }\mu\text{mol kg}^{-1}$. CO_2 concentration in seawater and the pH_{Total} (pH_{T}) values was calculated
107 by using CO2SYS (Pierrot et al., 2006) with the input of pH_{NBS} and TALK data.

108 **2.3 Nutrient measurement**

109 Surface seawater was collected from the Conductivity Temperature Depth (CTD)
110 rosette/Niskin bottles with a clean 125 mL HDPE (High-Density Polyethylene) sample
111 container. The nitrate and nitrite concentrations in seawater were then measured with a
112 Technicon AA3 Auto-Analyzer (Bran-Lube, GmbH, Germany). The quantitative limits
113 for nitrate and nitrite were $0.1\text{ }\mu\text{mol L}^{-1}$ and $0.04\text{ }\mu\text{mol L}^{-1}$, respectively. We used



114 certified reference materials (CRMS) (<https://www.jamstec.go.jp/scor/>) as external
115 quality checks, and the analytical precision was better than $\pm 1\%$ during the whole cruise.
116 Nutrient measurement was conducted in the cruise of the South China Sea basin. Due to
117 the limit of human resources, it was not conducted in the other two cruises.

118 **2.4 Solar radiation**

119 The incident solar radiation intensity during the cruises was recorded with an
120 Eldonet broadband filter radiometer (Eldonet XP, Real Time Computer, Germany). This
121 device has three channels for PAR (400–700 nm), UV-A (315–400 nm) and UV-B (280–
122 315 nm) irradiance, respectively, which records the means of solar radiations over each
123 minute. The instrument was fixed at the top layer of the ship to avoid shading.

124 **2.5 Determination of primary productivity**

125 Surface seawater (0-1m) was collected a 10 L acid-cleaned (1 M HCl) plastic bucket
126 and pre-filtered (200 μm mesh size) to remove large grazers. To prepare high CO_2 (HC)
127 seawater, CO_2 -saturated seawater was added into pre-filtered seawater until a decrease of
128 ~ 0.4 units in pH (corresponding CO_2 concentrations being 22.0-39.7 μM) was
129 approached (Gattuso et al., 2010). The same amount of filtered seawater (0.22 μm) was
130 added into the pre-filtered seawater setting as ambient CO_2 (AC) control. Prepared AC
131 and HC seawater was allocated into 50-mL quartz tubes in triplicate, inoculated with 5
132 μCi (0.185 MBq) $\text{NaH}^{14}\text{CO}_3$ (ICN Radiochemicals, USA), and then incubated for 24 h
133 (over a day-night cycle) under 100 % incident solar irradiances in a water bath for



134 temperature control by running through surface seawater. After the incubation, the cells
135 were filtered onto GF/F filters (Whatman) and immediately frozen at -20°C for later
136 analysis. In the laboratory, the frozen filters were transferred to 20 mL scintillation vials,
137 thawed and exposed to HCl fumes for 12 h, and dried (55°C , 6 h) to expel non-fixed ^{14}C ,
138 as previously reported (Gao et al., 2017). Then 3 mL scintillation cocktail (Perkin
139 Elmer®, OptiPhase HiSafe) was added to each vial. After 2 h of reaction, the
140 incorporated radioactivity was counted by a liquid scintillation counting (LS 6500,
141 Beckman Coulter, USA). The carbon fixation for 24 h incubation was taken as
142 chlorophyll (Chl) *a*-normalized daily net primary productivity (PP, $\mu\text{g C } (\mu\text{g Chl } a)^{-1}$)
143 (Gao et al., 2017). The changes (%) of PP induced by ocean acidification were expressed
144 as $(\text{PP}_{\text{HC}} - \text{PP}_{\text{AC}}) / \text{PP}_{\text{AC}} \times 100$, where PP_{HC} and PP_{AC} are the net daily primary productivity
145 under HC and AC, respectively.

146 **2.6 Chl *a* measurement**

147 Pre-filtered (200 μm mesh size) surface seawater (500-2000 mL) at each station was
148 filtered onto GF/F filter (25 mm, Whatman) and then stored at -80°C . After returning to
149 laboratory, phytoplankton cells on the GF/F filter were extracted overnight in absolute
150 methanol at 4°C in darkness. After centrifugation (5000 *g* for 10 min), the absorption
151 values of the supernatants were analyzed by a UV–VIS spectrophotometer (DU800,
152 Beckman, Fullerton, California, USA). The concentration of chlorophylls *a* (Chl *a*) was
153 calculated according to Porra (2002).



154 **2.7 Data analysis**

155 The data of environmental parameters were expressed in raw and the data of PP were
156 the means of triplicate incubations. Two-way analysis of variance (ANOVA) was used to
157 analyze the effects of OA and location on PP. Least significant difference (LSD) was used
158 to for *post hoc* analysis. Linear fitting analysis was conducted with Pearson correlation
159 analysis to assess the relationship between PP and environmental factors. A 95%
160 confidence level was used in all analyses.

161 **3 Results**

162 During the cruises, surface temperature ranged from 25.0 to 29.9 °C in the Taiwan
163 Strait and from 27.1 to 30.2 °C in the South China Sea (Fig. 2a). Surface salinity ranged
164 from 30.0 to 34.0 in the Taiwan Strait and from 31.0 to 34.3 in the South China Sea (Fig.
165 2b). The lower salinities were found in the estuaries of Minjiang and Jiulong Rivers as
166 well as Mekong River-induced Rip current. High salinities were found in the SCS basin.
167 Surface pH_T changed between 7.91-8.20 in the Taiwan Strait with the higher values in the
168 estuary of Minjiang River (Fig. 2c). On the contrary, surface pH had a narrower range
169 (8.06-8.23) in the South China Sea and the lower values occurred near the islands in the
170 Philippines. TALK ranged from 2100 to 2359 $\mu\text{mol L}^{-1}$ in the Taiwan Strait and 2126 to
171 2369 $\mu\text{mol L}^{-1}$ in the South China Sea (Fig. 2d). The lowest value occurred in the estuary
172 of Minjiang River. CO_2 concentration in surface seawater changed from 6.4-15.9 $\mu\text{M kg}^{-1}$
173 SW in the Taiwan Strait, and 9.3-14.3 $\mu\text{M kg}^{-1}$ SW in the SCS (Fig. 1e). It showed an



174 opposite pattern to surface pH, with the lowest value in the estuary of Minjiang River in
175 the Taiwan Strait and highest value in near the islands in the Philippines in the South
176 China Sea. During the PP investigation period, the daytime mean PAR intensity ranged
177 from 126.6 to 145.2 $\text{W m}^{-2} \text{s}^{-1}$ in the Taiwan Strait and 37.3 to 150.0 $\text{W m}^{-2} \text{s}^{-1}$ in the SCS
178 (Fig. 2f).

179 The concentration of Chl *a* ranged from 0.11 to 12.13 $\mu\text{g L}^{-1}$ in the Taiwan Strait (Fig.
180 3). The highest concentration occurred in the estuary of the Minjiang River. The
181 concentration of Chl *a* in the SCS ranged from 0.037 to 7.43 $\mu\text{g L}^{-1}$. The highest
182 concentration was found in the coastal areas of Guangdong province in China. For both
183 the Taiwan Strait and the SCS, there were high Chl *a* concentrations ($> 1.0 \mu\text{g L}^{-1}$) in
184 coastal areas, particularly in the estuaries of the Minjing River, Jiulong River and Pearl
185 River. On the contrary, Chl *a* concentrations in offshore areas were lower than 0.2 $\mu\text{g L}^{-1}$.

186 Surface primary productivity changed from 99-302 $\mu\text{g C } (\mu\text{g Chl } a)^{-1} \text{d}^{-1}$ in the
187 Taiwan Strait, and from 17-306 $\mu\text{g C } (\mu\text{g Chl } a)^{-1} \text{d}^{-1}$ in the South China Sea (Fig. 4).
188 High surface primary productivity ($> 200 \mu\text{g C } (\mu\text{g Chl } a)^{-1} \text{d}^{-1}$) was found in the
189 estuaries of the Minjing River, Jiulong River, and Pearl River and areas near the East of
190 Vietnam. In pelagic zones, the surface primary productivity was usually lower than 100
191 $\mu\text{g C } (\mu\text{g Chl } a)^{-1} \text{d}^{-1}$.

192 Through a series of onboard CO_2 -enrich experiments we observed that effects of the
193 elevated pCO_2 on primary productivity of surface phytoplankton community ranged from



194 -88.03% (inhibition) to 56.87% (promotion), revealing significant regional differences
195 (ANOVA, $F_{(100, 404)} = 4.103$, $p < 0.001$, Fig. 5). Among 101 stations, 70 stations showed
196 insignificant OA effects. OA increased PP at 6 stations and reduced PP at 25 stations.
197 Positive effects of OA on surface primary productivity was observed in the Taiwan Strait
198 and the western SCS (Fig. 5, red-yellow shading areas), with the maximal enhancement
199 of 56.9% in the station approaching Mekong River plume (LSD, $p < 0.001$). Reduction in
200 PP induced by the elevated CO₂ was mainly found in the central SCS basin within the
201 latitudes of 10 °N to 14 °N and the longitudes of 114.5 °E to 118 °E (Fig. 5, blue-purple
202 shading areas), with inhibition rates ranging from 24.02% to 88.03% (Fig. 5, LSD, $p <$
203 0.05). These results showed a region-related effect of OA on photosynthetic carbon
204 fixation of surface phytoplankton assemblages. Overall, the elevated pCO₂ had neutral or
205 positive effects on primary productivity in nearshore waters, while having adverse effects
206 in pelagic waters.

207 By analyzing the correlations between OA-induced PP changes and regional
208 environmental parameters, we found that OA-induced changes in phytoplankton primary
209 productivity was significantly positively related with *in situ* pH ($p < 0.001$, $r = 0.379$),
210 NO_x availability (the concentrations of NO₃⁻ + NO₂⁻ at the bottom of upper mixing layers
211 as they were unmeasurable in the surface water, $p = 0.002$, $r = 0.727$), PAR density ($p =$
212 0.002, $r = 0.311$) and primary productivity ($p = 0.004$, $r = 0.284$) (Fig. 6 and Table S1).
213 On the other hand, the influence induced by OA was negatively related to salinity that



214 ranged from 30.00 to 34.28 ($p < 0.001$, $r = -0.418$).

215 **4 Discussion**

216 In the present study, we found that the elevated pCO₂ and associated pH drop
217 increased or did not affect PP in coastal waters but reduced it in pelagic waters. Our
218 results suggested that the enhanced effects of the OA treatment on photosynthetic carbon
219 fixation depend on regions of different physicochemical conditions. Higher levels of
220 nutrients due to runoffs or upwellings should be mainly responsible for the enhancement.
221 On the other hand, such stimulation could be related to higher UV-attenuation in these
222 coastal waters that contain more organic matters (Hader et al., 2015), since we employed
223 UV-transparent vessels for the incubations. In addition, coastal diatoms appear to benefit
224 more from OA than pelagic ones (Li et al., 2016). Therefore, community structure
225 differences might also be responsible for the differences of the short-term high
226 CO₂-induced acidification between coastal and pelagic waters.

227 OA is deemed to have two kinds of effects at least (Xu et al., 2017; Shi et al., 2019).
228 The first one is the enrichment of CO₂, which is usually beneficial for photosynthetic
229 carbon fixation and growth of algae because insufficient ambient CO₂ limits algal
230 photosynthesis (Hein & Sand-Jensen, 1997; Bach & Taucher, 2019). The other effect is
231 the decreased pH which could be harmful because it disturbs the acid-base balance
232 between extracellular and intracellular environments. For instance, the decreased pH
233 projected for future OA was shown to reduce the growth of the diazotroph



234 *Trichodesmium* (Hong et al., 2017), decrease PSII activity by reducing removal rate of
235 PsbD (D2) (Gao et al., 2018b) and increase mitochondrial and photo-respirations in
236 diatoms and phytoplankton assemblages (Yang and Gao 2012, Jin et al., 2015). In
237 addition, OA could reduce the RuBisCO transcription of diatoms, which also contributed
238 to the decreased growth (Endo et al., 2015). Therefore, the net impact of OA depends on
239 the balance between its positive and negative effects, leading to enhanced, inhibited or
240 neutral influences, as reported in diatoms (Gao et al., 2012, Li et al., 2021) and
241 phytoplankton assemblages in the Arctic and subarctic shelf seas (Hoppe et al., 2018), the
242 North Sea (Eberlein et al., 2017) and the South China Sea (Wu and Gao 2010, Gao et al.,
243 2012).

244 In the present study, OA increased or did not affect PP in coastal waters but reduced
245 it in offshore waters. This is significantly related to nutrient availability (Fig. 6d), with
246 that the inhibitory effect was minimized when NO_x availability increased. Riverine
247 inputs, including the Minjiang River, Jiulong River, Pearl River, and Mekong River, are
248 the primary source of nutrients in the coastal and shelf zones, resulting in higher
249 concentrations of nutrients and lower salinity in these waters (Xiao et al., 2018). It was
250 reported that elevated pCO₂ decreased net organic carbon production of
251 natural plankton community in nutrient-depleted waters (Yoshimura et al., 2010).
252 Furthermore, OA did not affect the specific growth rate of a diatom under N-replete
253 condition but reduced it under N-limited condition (Li et al., 2018). The alleviating effect



254 of nutrient enrichment on OA-induced stress could be multifaceted. Firstly, algae could
255 cope with the acid-base perturbation caused by OA through active proton pumps
256 (McNicholl et al., 2019). The operation of such proton pumps need some essential
257 proteins, such as plasma membrane H⁺-ATPase, whose synthesis is nutrient-dependent
258 (Taylor et al., 2012; Xu et al., 2017). Secondly, it has been shown that nutrient
259 enrichment could accelerate the repair rate of PSII via synthesizing the key proteins such
260 as PsbA (D1), and PsbD (D2) (Geider et al., 1993; Li et al., 2015). Thirdly, nitrogen
261 enrichment could significantly increase the synthesis and content of photosynthetic
262 pigments including Chl *a*, phycocyanin, and phycoerythrin (Johnson & Carpenter, 2018;
263 Gao et al., 2019b), contributing to high photosynthetic activity under stressful
264 environmental conditions. Negative correlation between OA-induced changes of PP and
265 salinity was found in this study. While little has been documented on the relationship
266 between salinity and OA (Wulff et al., 2018; Sugie et al., 2020; Xu et al., 2020), lowered
267 salinity has been shown to alleviate the impact of OA on a coccolithorporid (Xu et al.,
268 2020). Nevertheless, we presume the enhanced PP could mainly be related to nutrient
269 availability because lower salinity in coastal waters usually companies with high nutrient
270 levels (Li et al., 2011). In addition, local pH may be another factor that affects the
271 impacts of OA. There are diurnal and seasonal fluctuations of pH in coastal waters and
272 phytoplankton that adapt well to the fluctuant pH environments would be tolerant to the
273 decreased pH caused by OA (Flynn et al., 2012, Li et al., 2016). On the other hand, the



274 surface pH in the ocean basin is relatively stable, with a varied range of only ~0.024 over
275 a month (Hofmann et al., 2011). Therefore, the phytoplankton cells living in these
276 environments could be more sensitive to pH drop due to elevated pCO₂ (Li et al., 2016).
277 The specific environmental conditions have profound effects on shaping diverse
278 dominant phytoplankton groups (Boyd et al., 2010). Larger eukaryotic groups (especially
279 diatoms) usually dominate the complex coastal regions, while picophytoplankton
280 (*Prochlorococcus* and *Synechococcus*), characterizing with more efficient nutrients
281 uptake, dominate the relatively stable offshore waters (Dutkiewicz et al., 2015). In
282 summer and early autumn, previous investigations demonstrated that diatoms dominated
283 in the northern waters and the Taiwan Strait (coastal and shelf regions) with the high
284 abundance of phytoplankton, which are consistent with our Chl *a* data; *Prochlorococcus*
285 and *Synechococcus* dominated in the SCS basin and the north of SCS (slope and basin
286 regions) (Xiao et al., 2018, Zhong et al., 2020). In addition, it has been reported that
287 larger cells benefit more from OA because a thicker diffusion layer around the cells limits
288 the transport of CO₂ (Feng et al., 2010; Wu et al., 2014). In contrast, a thinner diffusion
289 layer and higher surface to volume ratio in smaller phytoplankton cells can make them
290 easier to transport CO₂ near the cell surface and within the cells, and therefore
291 picophytoplankton species are less CO₂-limited (Bao and Gao, 2021). Therefore, different
292 community structures between coastal and pelagic areas could also be responsible for the
293 enhanced and inhibitory effects of OA.



294 **Conclusions**

295 By investigating the impacts of the elevated pCO₂ on PP in the Taiwan Strait and the
296 SCS, we demonstrated that such short OA-treatments induced changes in PP were mainly
297 related to NO_x availability based on Pearson correlation coefficients, supporting the
298 hypothesis that negative impacts of OA on PP increase from coastal to pelagic waters
299 (Gao et al., 2019a). In view of ocean climate changes, strengthened stratification due to
300 global warming would reduce the upward transports of nutrients and further reduce
301 nutrient availability, consequently, leading to exacerbating impacts of OA on PP in
302 pelagic zones. Meanwhile, PP in coastal and/or upwelled waters would be stimulated or
303 non-affected by OA with continuous discharges of nutrients from terrestrial environments,
304 which may imply higher PP and enhance frequency of harmful algal blooms in future
305 oceans.

306 *Data availability.* All data are included in the article or Supplement.

307 *Author contributions.* KG and TW developed the original idea and designed research.

308 TW and JS carried out fieldwork. GG provided statistical analyses and prepared figures.

309 GG, KG, and XZ wrote the manuscript. All contributed to revising the paper.

310 *Competing interests.* The contact author has declared that neither they nor their
311 co-authors have any competing interests.

312 *Disclaimer.* Publisher's note: Copernicus Publications remains neutral with regard to
313 jurisdictional claims in published maps and institutional affiliations.



314 *Acknowledgements.* This work was supported by the National Natural Science Foundation
315 of China (41720104005, 41890803 and 42076154), and the Fundamental Research Funds
316 for the Central Universities (20720200111). We appreciate the NFSC Shiptime Sharing
317 Project (project number: 41849901) for supporting the Taiwan Strait cruise
318 (NORC2016-04). We appreciate the chief scientists Yihua Cai, Huabin Mao and Chen Shi
319 and the R/V Yanping II, Shiyan I and Shiyan III for leading and conducting the cruises.

320 **References**

- 321 Bach, L. T., and Taucher, J.: CO₂ effects on diatoms: a synthesis of more than a decade of
322 ocean acidification experiments with natural communities, *Ocean Sci.*, 15,
323 1159-1175, 2019.
- 324 Bao, N., and Gao, K.: Interactive effects of elevated CO₂ concentration and light on the
325 picoplankton *Synechococcus*, *Front. Mar. Sci.*, 8, 1-7, 2021.
- 326 Boyd, P. W., Strzepek, R., Fu, F. X., and Hutchins, D. A.: Environmental control of open-
327 ocean phytoplankton groups: Now and in the future, *Limnol. Oceanogr.*, 55,
328 1353-1376, 2010.
- 329 Chen, C. T. A.: Rare northward flow in the Taiwan Strait in winter: A note, *Cont. Shelf*
330 *Res.*, 23, 387-391, 2003.
- 331 Cloern, J. E., Foster, S. Q. and Kleckner, A. E.: Phytoplankton primary production in the
332 world's estuarine-coastal ecosystems, *Biogeosciences*, 11, 2477-2501, 2014.
- 333 Doney, S. C., Busch, D. S., Cooley, S. R., and Kroeker, K. J.: The impacts of ocean



334 acidification on marine ecosystems and reliant human communities, *Annu. Rev. Env.*
335 *Resour.*, 45, 83-112, 2020.

336 Dutkiewicz, S., Morris, J. J., Follows, M. J., Scott, J., Levitan, O., Dyhrman, S. T., and
337 Berman-Frank, I.: Impact of ocean acidification on the structure of future
338 phytoplankton communities, *Nat. Clim. Change*, 5, 1002-1006, 2015.

339 Eberlein, T., Wohlrab, S., Rost, B., John, U., Bach, L. T., Riebesell, U., and Van de Waal,
340 D. B.: Effects of ocean acidification on primary production in a coastal North Sea
341 phytoplankton community, *Plos One*, 12, 1-15, 2017.

342 Endo, H., Sugie, K., Yoshimura, T., and Suzuki, K.: Effects of CO₂ and iron availability
343 on *rbcL* gene expression in Bering Sea diatoms, *Biogeosciences*, 12, 2247-2259,
344 2015.

345 Feng, Y., Hare, C. E., Rose, J. M., Handy, S. M., DiTullio, G. R., Lee, P. A., Smith, W. O.,
346 Peloquin, J., Tozzi, S., Sun, J., Zhang, Y., Dunbar, R. B., Long, M. C., Sohst, B.,
347 Lohan, M., and Hutchins, D. A.: Interactive effects of iron, irradiance and CO₂ on
348 Ross Sea phytoplankton, *Deep-Sea Res. PT. I*, 57, 368-383, 2010.

349 Flynn, K. J., Blackford, J. C., Baird, M. E., Raven, J. A., Clark, D. R., Beardall, J.,
350 Brownlee, C., Fabian, H., and Wheeler, G. L.: Changes in pH at the exterior surface
351 of plankton with ocean acidification, *Nat. Clim. Change*, 2, 510-513, 2012.

352 Gao, G., Xu, Z. G., Shi, Q., and Wu, H. Y.: Increased CO₂ exacerbates the stress of
353 ultraviolet radiation on photosystem II function in the diatom *Thalassiosira*



- 354 *weissflogii*, Environ. Exp. Bot., 156, 96-105, 2018b.
- 355 Gao, G., Gao, Q., Bao, M. L., Xu, J. T., and Li, X. S.: Nitrogen availability modulates the
356 effects of ocean acidification on biomass yield and food quality of a marine crop
357 *Pyropia yezoensis*, Food Chem, 271, 623-629, 2019b.
- 358 Gao, G., Jin, P., Liu, N., Li, F. T., Tong, S. Y., Hutchins, D. A., and Gao, K. S.: The
359 acclimation process of phytoplankton biomass, carbon fixation and respiration to the
360 combined effects of elevated temperature and $p\text{CO}_2$ in the northern South China Sea,
361 Mar. Pollut. Bull., 118, 213-220, 2017.
- 362 Gao, G., Xia, J. R., Yu, J. L., Fan, J. L., and Zeng, X. P.: Regulation of inorganic carbon
363 acquisition in a red tide alga (*Skeletonema costatum*): The importance of phosphorus
364 availability, Biogeosciences, 15, 4871-4882, 2018a.
- 365 Gao, K. S., Beardall, J., Häder, D. P., Hall-Spencer, J. M., Gao, G., and Hutchins, D. A.:
366 Effects of ocean acidification on marine photosynthetic organisms under the
367 concurrent influences of warming, UV radiation, and deoxygenation, Front. Mar.
368 Sci., 6, 1-18, 2019a.
- 369 Gao, K. S., Xu, J. T., Gao, G., Li, Y. H., Hutchins, D. A., Huang, B. Q., Wang, L., Zheng,
370 Y., Jin, P., Cai, X. N., Hader, D. P., Li, W., Xu, K., Liu, N. N., and Riebesell, U.:
371 Rising CO_2 and increased light exposure synergistically reduce marine primary
372 productivity, Nat. Clim. Change, 2, 519-523, 2012.
- 373 Gattuso, J. P., Gao, K. S., Lee, K., Rost, B., and Schulz, K. G.: Approaches and tools to



374 manipulate the carbonate chemistry, pp 41-52. Guide to best practices for ocean
375 acidification research and data reporting, edited by: Riebesell, U., Fabry, V. J.,
376 Hansson, L., and Gattuso J.-P., Luxembourg: Publications Office of the European
377 Union, 2010.

378 Gattuso, J. P., Magnan, A., Billé R., Cheung, W. W. L., Howes, E. L., Joos, F., Allemand,
379 D., Bopp, L., Cooley, S. R., Eakin, C. M., Hoegh-Guldberg, O., Kelly, R. P., Portner,
380 H. O., Rogers, A. D., Baxter, J. M., Laffoley, D., Osborn, D., Rankovic, A., Rochette,
381 J., Sumaila, U. R., Treyer, S., and Turley, C.: Contrasting futures for ocean and
382 society from different anthropogenic CO₂ emissions scenarios, *Science*, 349,
383 aac4722, 2015.

384 Geider, R. J., La Roche, J., Greene, R. M., and Olaizola, M.: Response of the
385 photosynthetic apparatus of *Phaeodactylum tricornutum* (Bacillariophyceae) to
386 nitrate, phosphate, or iron starvation, *J. Phycol.*, 29, 755-766, 1993.

387 Häder, D. P., Williamson, C. E., Wängberg, S. A., Rautio, M., Rose, K. C., Gao, K. S.,
388 Helbling, E. W., Sinha, R. P., and Worrest, R.: Effects of UV radiation on aquatic
389 ecosystems and interactions with other environmental factors, *Photoch. Photobio.*
390 *Sci.*, 14, 108-126, 2015.

391 Hedges, J. I., and Keil, R. G.: Sedimentary organic matter preservation: an assessment
392 and speculative synthesis, *Mar. Chem.*, 49, 81-115, 1995.

393 Hein, M., and Sand-Jensen, K.: CO₂ increases oceanic primary production, *Nature*, 388,



- 394 526-527, 1997.
- 395 Hennon, G. M. M., Ashworth, J., Groussman, R. D., Berthiaume, C., Morales, R. L.,
396 Baliga, N. S., Orellana, M. V., and Armbrust, E. V.: Diatom acclimation to elevated
397 CO₂ via cAMP signalling and coordinated gene expression, *Nat. Clim. Change*, 5,
398 761-765, 2015.
- 399 Hofmann, G. E., Smith, J. E., Johnson, K. S., Send, U., Levin, L. A., Micheli, F., Paytan,
400 A., Price, N. N., Peterson, B., Takeshita, Y., Matson, P. G., Crook, E. D., Kroeker, K.
401 J., Gambi, M. C., Rivest, E. B., Frieder, C. A., Yu, P. C., and Martz, T. R.:
402 High-frequency dynamics of ocean pH: A multi-ecosystem comparison, *Plos One*, 6,
403 1-11, 2011.
- 404 Holding, J. M., Duarte, C. M., Sanz-Martín, M., Mesa, E., Arrieta, J. M., Chierici, M.,
405 Hendriks, I. E., Garcia-Corral, L. S., Regaudie-de-Gioux, A., Delgado, A., Reigstad,
406 M., Wassmann, P., and Agusti, S.: Temperature dependence of CO₂-enhanced
407 primary production in the European Arctic Ocean, *Nat. Clim. Change*, 5, 1079-1082,
408 2015.
- 409 Hong, H. S., Chai, F., Zhang, C. Y., Huang, B. Q., Jiang, Y. W., and Hu, J. Y.: An
410 overview of physical and biogeochemical processes and ecosystem dynamics in the
411 Taiwan Strait, *Cont. Shelf Res.*, 31, S3-S12, 2011.
- 412 Hong, H. Z., Shen, R., Zhang, F. T., Wen, Z. Z., Chang, S. W., Lin, W. F., Kranz, S. A.,
413 Luo, Y. W., Kao, S. J., Morel, F. M. M. and Shi, D. L.: The complex effects of ocean



- 414 acidification on the prominent N₂-fixing cyanobacterium *Trichodesmium*. *Science*,
415 356, 527-530, 2017.
- 416 Hopkinson, B. M., Dupont, C. L., Allen, A. E., and Morel, F. M.: Efficiency of the
417 CO₂-concentrating mechanism of diatoms, *P. Natl. Acad. Sci. USA.*, 108, 3830-3837,
418 2011.
- 419 Hoppe, C. J. M., Wolf, K. K. E., Schuback, N., Tortell, P. D., and Rost, B.: Compensation
420 of ocean acidification effects in Arctic phytoplankton assemblages. *Nat. Clim.*
421 *Change*, 8, 529-533, 2018.
- 422 Jin, P., Gao, G., Liu, X., Li, F. T., Tong, S. Y., Ding, J. C., Zhong, Z. H., Liu, N. N., and
423 Gao, K. S.: Contrasting photophysiological characteristics of phytoplankton
424 assemblages in the Northern South China Sea, *Plos One*, 11, 1-16, 2016.
- 425 Jin, P., Wang, T. F., Liu, N. N., Dupont, S., Beardall, J., Boyd, P. W., Riebesell, U., and
426 Gao, K. S.: Ocean acidification increases the accumulation of toxic phenolic
427 compounds across trophic levels, *Nat. Commun.*, 6, 1-6, 2015.
- 428 Johnson, M. D., and Carpenter, R. C.: Nitrogen enrichment offsets direct negative effects
429 of ocean acidification on a reef-building crustose coralline alga, *Biol. Letters*, 14,
430 1-5, 2018.
- 431 Lan, J., Hong, J. and Li, P.: Seasonal variability of cool-core eddy in the Western South
432 China Sea, *Adv. Earth Sci.*, 21, 1145-1152, 2006.
- 433 Li, F. T., Wu, Y. P., Hutchins, D. A., Fu, F. X., and Gao, K. S.: Physiological responses of



- 434 coastal and oceanic diatoms to diurnal fluctuations in seawater carbonate chemistry
435 under two CO₂ concentrations, *Biogeosciences*, 13, 6247-6259, 2016.
- 436 Li, F. T., Beardall, J., and Gao, K. S.: Diatom performance in a future ocean: interactions
437 between nitrogen limitation, temperature, and CO₂-induced seawater acidification,
438 *ICES J. Mar. Sci.*, 75, 1451-1464, 2018.
- 439 Li, G., Gao, K. S., Yuan, D. X., Zheng, Y., and Yang, G. Y.: Relationship of
440 photosynthetic carbon fixation with environmental changes in the Jiulong River
441 estuary of the South China Sea, with special reference to the effects of solar UV
442 radiation, *Mar. Pollut. Bull.*, 62, 1852-1858, 2011.
- 443 Li, H. X., Xu, T. P., Ma, J., Li, F. T., and Xu, J. T.: Physiological responses of
444 *Skeletonema costatum* to the interactions of seawater acidification and the
445 combination of photoperiod and temperature, *Biogeosciences*, 18, 1439-1449, 2021.
- 446 Li, W., Gao, K., and Beardall, J.: Nitrate limitation and ocean acidification interact with
447 UV-B to reduce photosynthetic performance in the diatom *Phaeodactylum*
448 *tricornutum*, *Biogeosciences*, 12, 2383-2393, 2015.
- 449 McNicholl, C., Koch, M. S., and Hofmann, L. C.: Photosynthesis and light-dependent
450 proton pumps increase boundary layer pH in tropical macroalgae: A proposed
451 mechanism to sustain calcification under ocean acidification, *J. Exp. Mar. Biol.*
452 *Ecol.*, 521, 1-12, 2019.
- 453 Mostofa, K.M., Liu, C.Q., Zhai, W., Minella, M., Vione, D., Gao, K., Minakata, D.,



- 454 Arakaki, T., Yoshioka, T., Hayakawa, K. and Konohira, E.: Reviews and Syntheses:
455 Ocean acidification and its potential impacts on marine ecosystems, *Biogeosciences*,
456 13, 1767-1786, 2016.
- 457 Pierrot, D., Wallace, D.W. R., and Lewis, E.: MS Excel program developed for CO₂
458 system calculations. ORNL/CDIAC-105a, Carbon Dioxide Information Analysis
459 Center, Oak Ridge National Laboratory, US Department of Energy, Oak Ridge,
460 Tennessee, USA., 2006.
- 461 Porra, R. J.: The chequered history of the development and use of simultaneous equations
462 for the accurate determination of chlorophylls a and b, *Photosynth. Res.*, 73,
463 149-156, 2002.
- 464 Raven, J. A., and Beardall, J.: CO₂ concentrating mechanisms and environmental change,
465 *Aquat. Bot.*, 118, 24-37, 2014.
- 466 Schippers, P., Lüring, M., and Scheffer, M.: Increase of atmospheric CO₂ promotes
467 phytoplankton productivity, *Ecol. Lett.*, 7, 446-451, 2004.
- 468 Shi, D. L., Hong, H. Z., Su, X., Liao, L. R., Chang, S. W., and Lin, W. F.: The
469 physiological response of marine diatoms to ocean acidification: Differential roles of
470 seawater *p*CO₂ and pH, *J. Phycol.*, 55, 521-533, 2019.
- 471 Sugie, K., Fujiwara, A., Nishino, S., Kameyama, S. and Harada, N.: Impacts of
472 temperature, CO₂, and salinity on phytoplankton community composition in the
473 Western Arctic Ocean, *Front. Mar. Sci.*, 6, 1-17, 2020.



- 474 Taylor, A. R., Brownlee, C., and Wheeler, G. L.: Proton channels in algae: Reasons to be
475 excited, *Trends Plant Sci.*, 17, 675-684, 2012.
- 476 Tortell, P. D., Rau, G. H., and Morel, F. M. M.: Inorganic carbon acquisition in coastal
477 Pacific phytoplankton communities, *Limnol. Oceanogr.*, 45, 1485-1500, 2000.
- 478 Tremblay, J. E., Michel, C., Hobson, K. A., Gosselin, M., and Price, N. M.: Bloom
479 dynamics in early opening waters of the Arctic Ocean. *Limnol. Oceanogr.*, 51,
480 900-912, 2006.
- 481 Riebesell, U., Aberle-Malzahn, N., Achterberg, E. P., Algueró-Muñiz, M.,
482 Alvarez-Fernandez, S., Arístegui, J., Bach, L. T., Boersma, M., Boxhammer, T.,
483 Guan, W. C., Haunost, M., Horn, H. G., Loscher, C. R., Ludwig, A., Spisla, C.,
484 Sswat, M., Stange, P., and Taucher, J.: Toxic algal bloom induced by ocean
485 acidification disrupts the pelagic food web, *Nat. Clim. Change*, 8, 1082-1086, 2018.
- 486 Wu, Y., Gao, K., and Riebesell, U.: CO₂-induced seawater acidification affects
487 physiological performance of the marine diatom *Phaeodactylum tricorutum*,
488 *Biogeosciences*, 7, 2915-2923, 2010.
- 489 Wu, Y., Campbell, D. A., Irwin, A. J., Suggett, D. J., and Finkel, Z. V.: Ocean
490 acidification enhances the growth rate of larger diatoms. *Limnol. Oceanogr.*, 59,
491 1027-1034, 2014.
- 492 Wu, Y. P., and Gao, K. S.: Combined effects of solar UV radiation and CO₂-induced
493 seawater acidification on photosynthetic carbon fixation of phytoplankton



- 494 assemblages in the South China Sea. *Chinese Sci. Bull.*, 55, 3680-3686, 2010.
- 495 Wulff, A., Karlberg, M., Olofsson, M., Torstensson, A., Riemann, L., Steinhoff, F. S.,
496 Mohlin, M., Ekstrand, N., and Chierici, M.: Ocean acidification and desalination:
497 Climate-driven change in a Baltic Sea summer microplanktonic community, *Mar.*
498 *Biol.*, 165, 1-15, 2018.
- 499 Xiao, W. P., Wang, L., Laws, E., Xie, Y. Y., Chen, J. X., Liu, X., Chen, B. Z., and Huang,
500 B. Q.: Realized niches explain spatial gradients in seasonal abundance of
501 phytoplankton groups in the South China Sea, *Prog. Oceanogr.*, 162, 223-239, 2018.
- 502 Xu, J. K., Sun, J. Z., Beardall, J., and Gao, K. S.: Lower salinity leads to improved
503 physiological performance in the coccolithophorid *Emiliana huxleyi*, which partly
504 ameliorates the effects of ocean acidification, *Front. Mar. Sci.*, 7, 1-18, 2020.
- 505 Xu, Z. G., Gao, G., Xu, J. T., and Wu, H. Y.: Physiological response of a golden tide alga
506 (*Sargassum muticum*) to the interaction of ocean acidification and phosphorus
507 enrichment, *Biogeosciences*, 14, 671-681, 2017.
- 508 Yang, G. Y., and Gao, K. S.: Physiological responses of the marine diatom *Thalassiosira*
509 *pseudonana* to increased $p\text{CO}_2$ and seawater acidity, *Mar. Environ. Res.*, 79,
510 142-151, 2012.
- 511 Yoshimura, T., Nishioka, J., Suzuki, K., Hattori, H., Kiyosawa, H. and Watanabe, Y. W.:
512 Impacts of elevated CO_2 on organic carbon dynamics in nutrient depleted Okhotsk
513 Sea surface waters. *J. Exp. Mar. Biol. Ecol.*, 395, 191-198, 2010.



514 Zhong, Y. P., Liu, X., Xiao, W. P., Laws, E. A., Chen, J. X., Wang, L., Liu, S. G., Zhang,
515 F., and Huang, B. Q.: Phytoplankton community patterns in the Taiwan Strait match
516 the characteristics of their realized niches, *Prog. Oceanogr.*, 186, 1-15, 2020.



517 **Figure captions**

518 **Fig. 1** Sampling stations for the incubation experiments in the Taiwan Strait and the
519 South China Sea during three cruises. Taiwan Strait cruise was conducted in July 2016
520 (red dots), South China Sea Basin cruise were conducted in September 2016 (blue dots)
521 and Western South China Sea cruise was conducted in September 2017 (black dots). The
522 arrows represent surface circulation fields in summer in the vicinity of Vietnam coast
523 based on Lan et al. (2006).

524 **Fig. 2** Temperature ($^{\circ}\text{C}$, panel a), salinity (panel b), pH (panel c), total alkalinity (μmol
525 L^{-1} , panel d), and CO_2 ($\mu\text{mol kg}^{-1}$ SW, panel e) in surface seawater and mean PAR
526 intensity ($\text{W m}^{-2} \text{s}^{-1}$, panel f) during the PP incubation experiments.

527 **Fig. 3** Chl *a* concentration ($\mu\text{g L}^{-1}$) in the Taiwan Strait and the South China Sea during
528 research cruises.

529 **Fig. 4** Surface primary productivity ($\mu\text{g C } (\mu\text{g Chl } a)^{-1} \text{ d}^{-1}$) in the Taiwan Strait and the
530 South China Sea during research cruises.

531 **Fig. 5** Ocean acidification (pH decreases of 0.4 units) induced changes (%) of surface
532 primary productivity in the Taiwan Strait and the South China Sea. Red-yellow shading
533 represents a positive effect on PP and blue-purple shading represents a negative effect.
534 Positive effect was found in coastal waters and estuary affected waters, such as the
535 Taiwan Strait, the Pearl River plume, Mekong River induced Rip current in West China
536 Sea. Negative effect was found in surface of oligotrophic waters like SCS Basin.



Fig. 6 Ocean acidification (pH decreases of 0.4 units) induced changes (%) on surface primary productivity in the South China Sea as a function of salinity (a), PAR (b), ambient pH (c), and nitrate plus nitrite concentration (d). The dotted lines represent 95% confidence intervals.

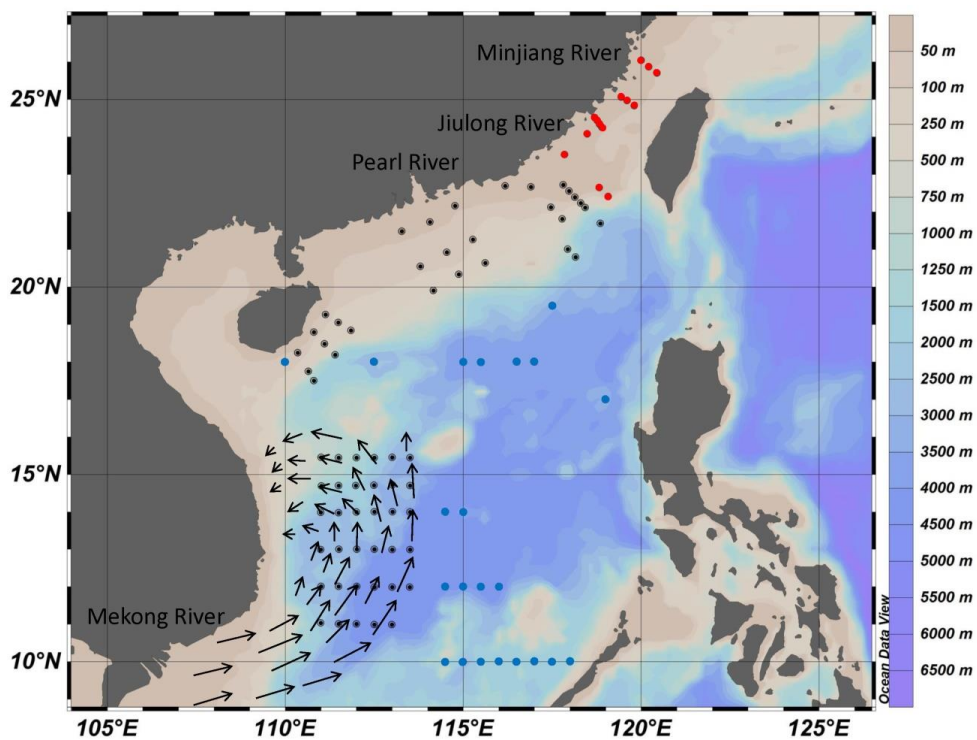


Fig. 1

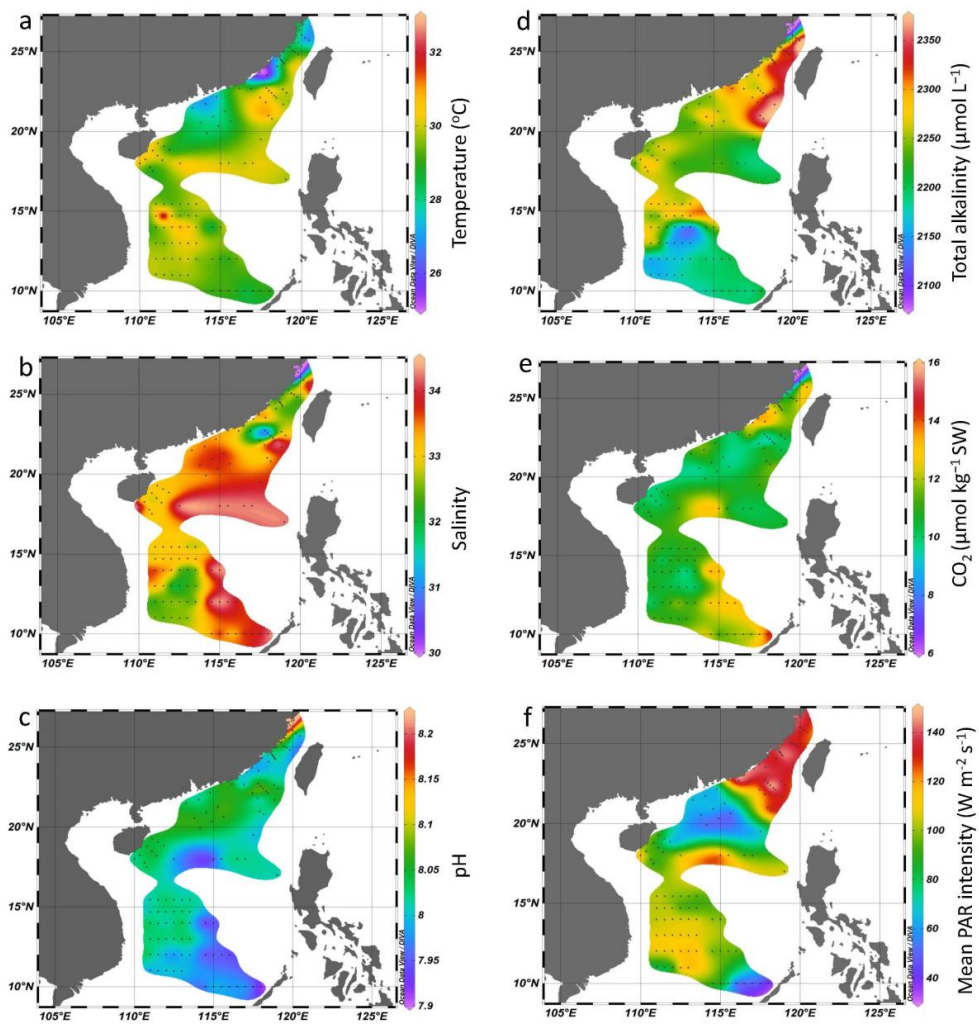


Fig. 2

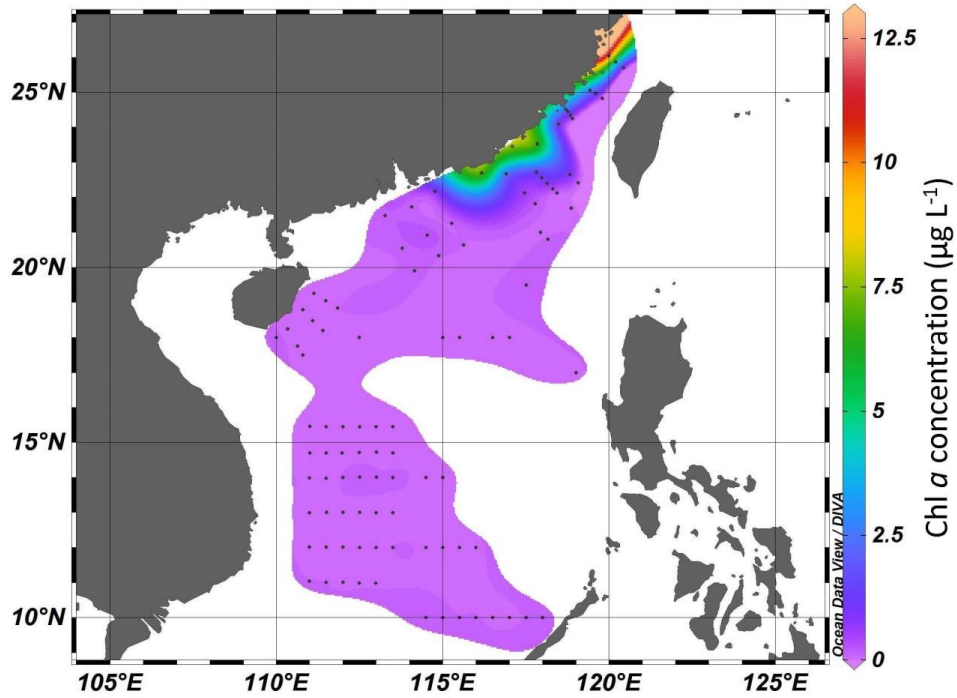


Fig. 3

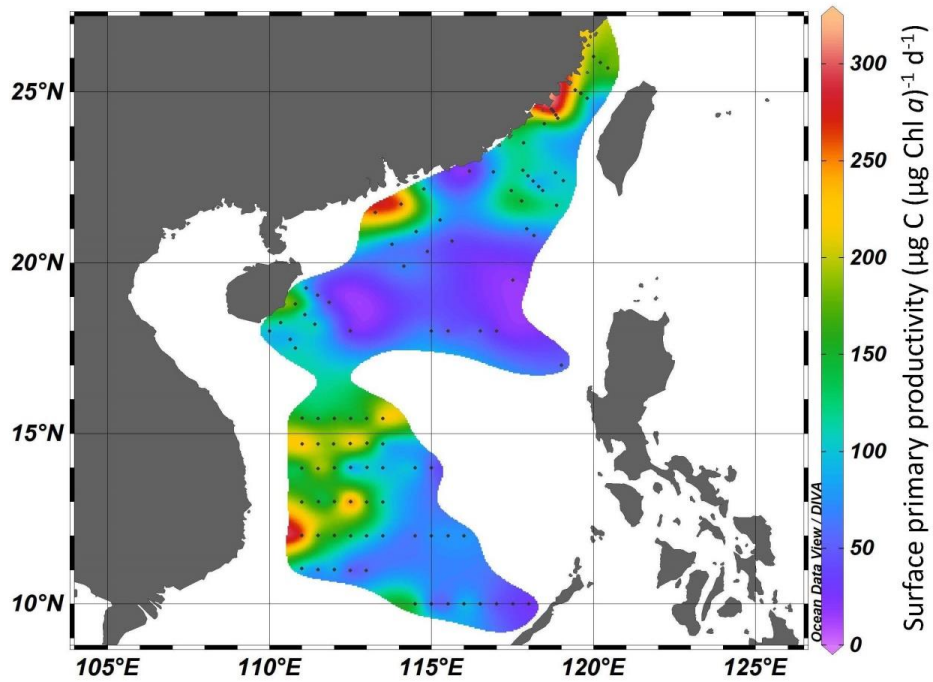


Fig. 4

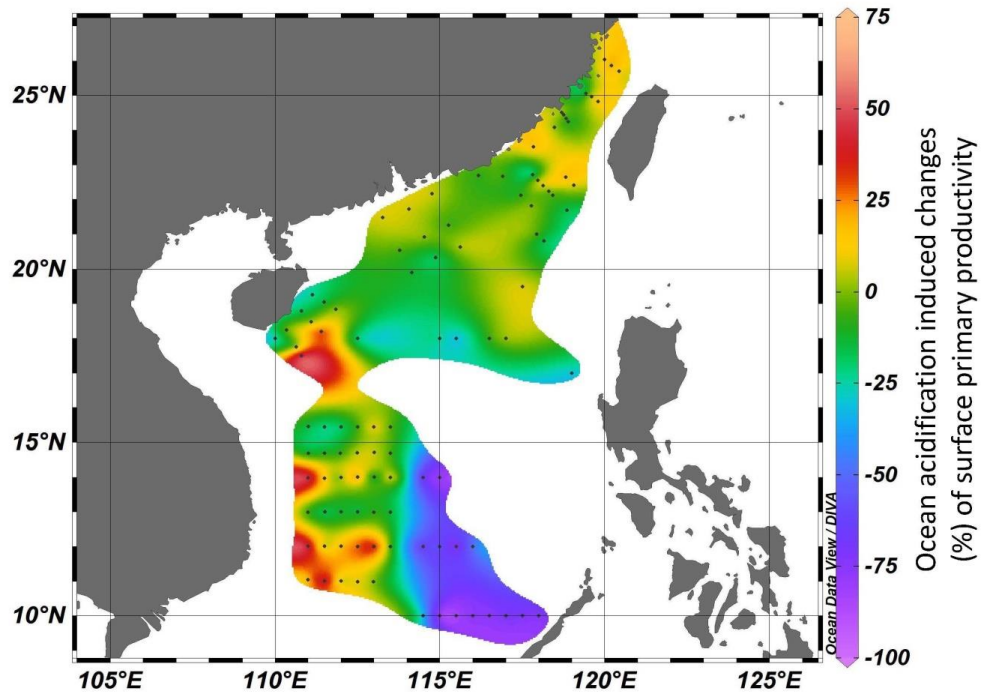


Fig. 5

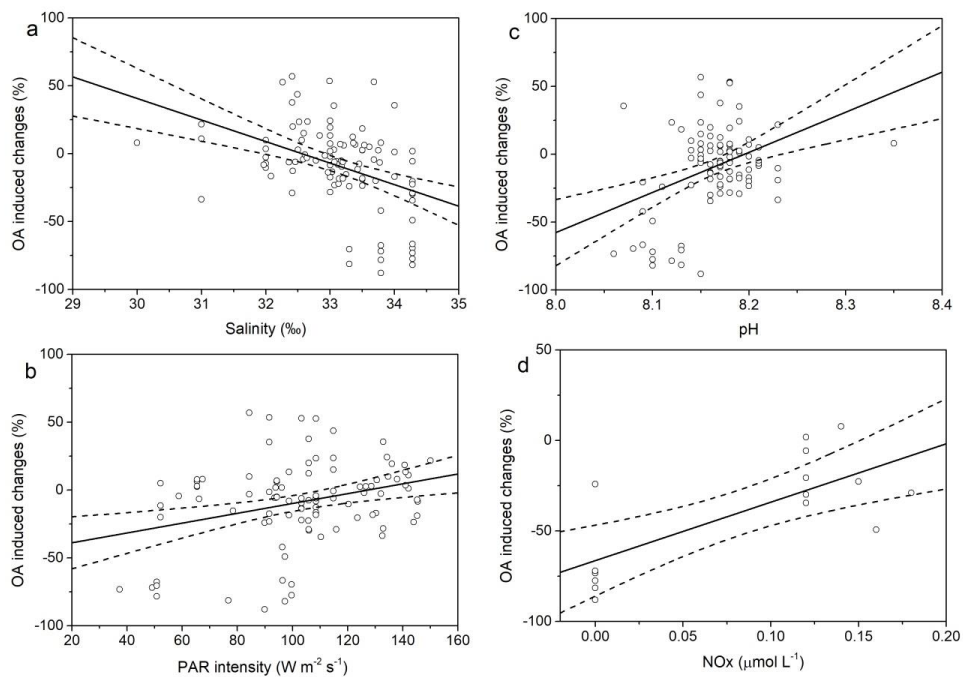


Fig. 6